



Cite this: *RSC Adv.*, 2019, 9, 35059

# Multifunctional lubricant additive based on difluoroboron derivatives of a diphenylamine antioxidant†

Shengpei Wang,<sup>ab</sup> Shasha Yu,<sup>ab</sup> Jianxiang Feng<sup>a</sup> and Shenggao Liu<sup>\*a</sup>

A metal-free and phosphorus-free novel multifunctional additive (*E*)-4-((3-*tert*-butyl)-2-((difluoroboranyl)oxy)-5-((octylthio)methyl)benzylidene)amino)-*N*-phenylaniline (difluoroboron derivative **4a**) was synthesized and characterized. The results show that its antioxidation and tribological properties are better than those of base oil, diphenylamine and zinc dialkyldithiophosphate (ZDDP), and it can also increase the extreme pressure performance of the base oil. In addition, it can be found that the diphenylamine functional group, boron and fluorine are the main contributors to the excellent antioxidation and antiwear properties of difluoroboron derivative **4a**, respectively. Finally, the results of X-ray photoelectron spectroscopy on the worn surfaces reveal that B<sub>2</sub>O<sub>3</sub>, Fe<sub>2</sub>O<sub>3</sub>, a N-containing organic compound and iron fluoride comprise the boundary films, which effectively improve the difluoroboron derivative **4a**'s antiwear properties.

Received 17th July 2019  
 Accepted 16th October 2019

DOI: 10.1039/c9ra05490a

[rsc.li/rsc-advances](http://rsc.li/rsc-advances)

## 1. Introduction

In order to reduce wear and friction and prolong the service life of mechanical systems, lubricants are widely used in industry.<sup>1</sup> Multifunctional lubricant additives are a kind of lubricant additive with more than one property.<sup>2</sup> Zinc dialkyldithiophosphate (ZDDP) is the most widely used multifunctional lubricant additive with excellent antioxidation, anticorrosive and antiwear abilities.<sup>3</sup> However, SAPS (Sulfated ash, Phosphorous and Sulfur) of ZDDP are prone to reduce the life of automotive exhaust gas-treatment systems. In order to improve the compatibility of the emission system, strict laws restrict the use of ZDDP.<sup>4,5</sup> For example, ILSAC GF-5 standards limit the phosphorous and sulfur contents in vehicle engine oil below 0.08% and 0.50%, respectively.<sup>6</sup> Therefore, it is a progressive trend to develop new non-SAPS or low SAPS multifunctional lubricant additives without reducing the antioxidation and antiwear capabilities.<sup>7–9</sup>

Several kinds of compounds with low or zero SAPS has been studied, such as heterocyclic compounds,<sup>10–12</sup> boron containing compounds,<sup>13–15</sup> ionic liquids<sup>16,17</sup> and nanoparticles.<sup>18–20</sup> It is well known that antioxidants can improve the oxidation stability of lubricant. Modification of antioxidants with the active elements of B, S and P is a research hotspot of

multifunctional lubricant additives, such as multifunctional Schiff bases (e.g. **CySBE** and **TrBzEd**),<sup>21–24</sup> high performance multifunctional additive **BHMT**,<sup>10</sup> N-containing borate ester **BMEB** (ref. 25) and imidazolium-based ionic liquids (e.g. **(BHT-1)MIMBF<sub>4</sub>**).<sup>26,27</sup> As shown in Scheme 1, all the above works focus on the modification of hindered phenolic antioxidants. Diphenylamine has been widely used as the main free radical scavenger, but there are few multifunctional additives synthesized by modifying diphenylamine. Weimin Liu and co-authors have synthesized some novel multifunctional additives **P-N compounds** (Scheme 1) with better tribological behaviors than ZDDP.<sup>2</sup> However, due to the removal of active H atom in diphenylamine, their antioxidation capacity is not significantly better than ZDDP. So, it is meaningful and challenging to synthesize a new high performance and low or zero SAPS multifunctional additive by modifying diphenylamine.

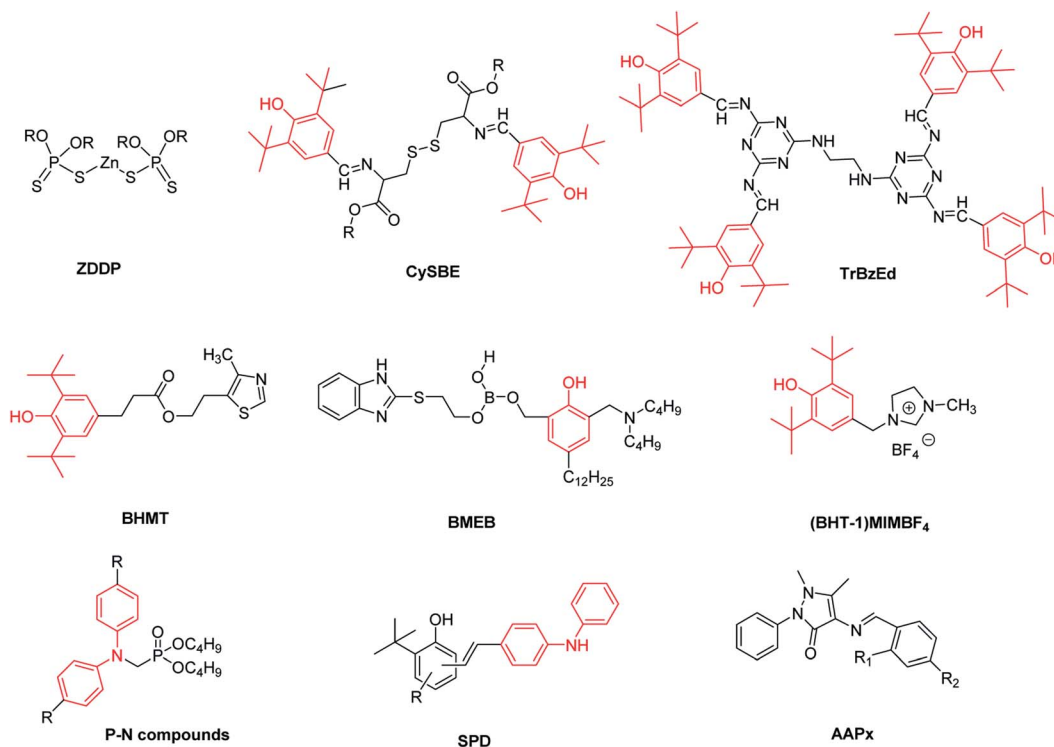
Recently, we have synthesized a series of Schiff base bridged phenolic diphenylamine (**SPD**, Scheme 1) antioxidants, which have better antioxidation performance than commercial antioxidants.<sup>28,29</sup> It is interesting that synergistic antioxidation effect was found when combined with borate polyisobutylene succinimide (PIBSI) dispersant.<sup>28</sup> Furthermore, it has been reported that the antiwear properties of lubricating oils can be greatly improved by the mixture or chemical synthesis of the Schiff bases (such as **AAPx** in Scheme 1) and borate esters.<sup>30–32</sup> Thus, based on the great synergistic effect between Schiff base and borate, we designed and synthesized a new kind of coordinately saturated boron complex by combining N<sup>^</sup>O-bidentate ligands in **SPD** with B(III) fragment. Unlike the reported borate ester additives, BF<sub>2</sub> was selected as the B(III) fragment due to the antiwear performance of fluorine containing compounds,<sup>26,33</sup> facile synthesis and stable

<sup>a</sup>Ningbo Institute of Materials Technology and Engineering, Chinese Academy of Sciences, No. 1219, Zhongguan West Road, Ningbo, Zhejiang, 315201, P. R. China. E-mail: [rukawayss@hotmail.com](mailto:rukawayss@hotmail.com); [sliu@nimte.ac.cn](mailto:sliu@nimte.ac.cn)

<sup>b</sup>University of Chinese Academy of Sciences, Beijing, 100049, P. R. China

† Electronic supplementary information (ESI) available. See DOI: 10.1039/c9ra05490a





Scheme 1 The structures of the related multifunctional additives and Schiff base compounds.

structure similar to Boranil complexes.<sup>34,35</sup> The antioxidation and antiwear performances of the difluoroboron derivatives of **SPD** antioxidants as multifunctional additives were evaluated and discussed. To our delight, compared with the traditional **ZDDP** and the commercial antioxidant diphenylamine (DPA), the selected additive (*E*)-4-((3-(*tert*-butyl)-2-((difluoroboranyl)oxy)-5-((octylthio)methyl)benzylidene)amino)-*N*-phenylaniline (difluoroboron derivative **4a**) has better wear resistance and oxidation resistance. As far as we know, this is the first time that boron, fluorine and diphenylamine antioxidants **SPD** have been combined to form a new non-phosphorus and non-metal compound as a potential multifunctional additive for lubricant.

## 2. Materials and experimental section

### 2.1. Materials

Solvents, reagents and DPA were bought from commercial sources. Polyisobutylene succinimide dispersant (PIBSI) was prepared according to the patent.<sup>36</sup> And T203 (zinc diisooctyl dithiophosphate) was obtained as a gift and chosen to represent **ZDDP**. Commercial mineral oil 150N was purchased from China National Offshore Oil Corporation. The physico-chemical properties of T203 and 150N are listed in Table 1.

### 2.2. Characterization

All NMR spectra (<sup>1</sup>H, <sup>13</sup>C, <sup>11</sup>B, <sup>19</sup>F) were recorded on Bruker AVANCE-400 MHz spectrometer at room temperature. High resolution mass spectra (HRMS) and element contents were analyzed by UPLC-Q-TOF mass spectrometer (AB Sciex TripleTOF

4600 system) and ICP-OES (SPECTRO ARCOS), respectively. The surface features and energy dispersive X-ray spectroscopy (EDS) of the worn scars were probed by scanning electron microscope (SEM) measurements (EVO18, Zeiss, Germany). The results of X-ray photoelectron spectroscopy (XPS) were acquired on imaging photoelectron spectrometer (AXIS ULTRA).

### 2.3. Synthesis and characterization of the compounds

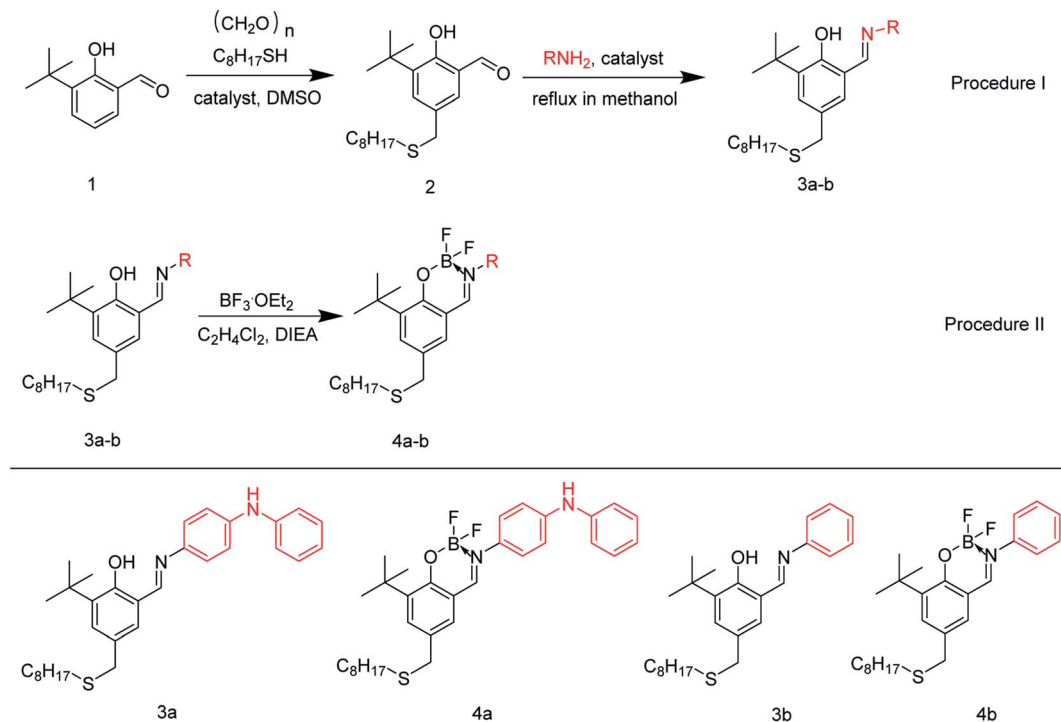
The synthesis process is shown in Scheme 2 and ESI Section S1.1.†

**2.3.1. Synthesis of (*E*)-2-(*tert*-butyl)-4-((octylthio)methyl)-6-(((4-(phenylamino)phenyl)imino)methyl)phenol (Schiff base **3a**).** Schiff base **3a** as an antioxidant has been synthesized and studied in our previous works.<sup>29</sup> As an important reaction intermediate and reference material in this study, it was synthesized according to general procedure I of Scheme 2 and ESI Section S1.1.†

Table 1 Properties of T203 and 150N

Item	T203	150N
Kinematic viscosity (40 °C), mm <sup>2</sup> s <sup>-1</sup>	—	27.9
Kinematic viscosity (100 °C), mm <sup>2</sup> s <sup>-1</sup>	—	5.2
Flash point, °C	>190	238.1
Water content, wt%	0.03	0.0073
Sulfur content, wt%	15.04	<0.0001
Phosphorus content, wt%	7.61	—
Zinc content, %	9.02	—
Density, 20 °C, kg m <sup>-3</sup>	1096.1	840





Scheme 2 Synthesis processes of Schiff bases and difluoroboron derivatives.

**2.3.2. Synthesis of (*E*)-4-((3-(*tert*-butyl)-2-((difluoroboranyl)oxy)-5-((octylthio)methyl)benzylidene)amino)-*N*-phenylaniline (difluoroboron derivative 4a).** The synthesis follows general procedure II of Scheme 2 and ESI Section S1.1.† Starting material: Schiff base 3a. Product: yellow solid. Isolated yield: 85% (3 g). <sup>1</sup>H NMR (Fig. S1,† 400 MHz, DMSO) δ 9.05 (s, 1H), 8.59 (s, 1H), 7.75–6.76 (m, 11H), 3.74 (s, 2H), 2.42 (t, *J* = 7.2 Hz, 2H), 1.55–1.13 (m, 21H), 0.84 (t, *J* = 6.5 Hz, 3H). <sup>13</sup>C NMR (Fig. S2,† 101 MHz, DMSO) δ 163.72 (s), 156.25 (s), 144.97 (s), 142.74 (s), 138.51 (s), 136.02 (s), 133.89 (s), 131.10 (s), 130.45 (s), 129.76 (s), 124.81 (s), 121.33 (s), 118.42 (s), 116.92 (s), 116.34 (s), 34.96 (d, *J* = 2.4 Hz), 31.69 (s), 31.13 (s), 29.50 (s), 29.25 (s), 29.08 (s), 29.02 (s), 28.70 (s), 22.52 (s), 14.37 (s). <sup>11</sup>B NMR (Fig. S3,† 128 MHz, DMSO) δ 94.33 (s). <sup>19</sup>F NMR (Fig. S4,† 377 MHz, DMSO) δ –133.77 (d, *J* = 23.8 Hz). HRMS (Fig. S5†) found for C<sub>32</sub>H<sub>41</sub>BF<sub>2</sub>N<sub>2</sub>OS [M – H]<sup>–</sup>: 549.3001, calcd: 549.2997. Elemental analysis, S: 5.57% (calcd: 5.82%); B: 1.86% (calcd: 1.96%). The sulfur content of difluoroboron derivative 4a is lower than that of ZDDP (e.g. T203 is 15%).

**2.3.3. Synthesis of (*E*)-1-(3-(*tert*-butyl)-2-((difluoroboranyl)oxy)-5-((octylthio)methyl)phen-yl)-*N*-phenylmethanimine (difluoroboron derivative 4b).** Schiff base 3b was synthesized by substituting *p*-aminodiphenylamine with aniline in accordance with general procedure I and ESI Section S1.† Then difluoroboron derivative 4b was obtained by general procedure II and ESI Section S1.1.† Product: yellow oil. Isolated yield: 80% (2 g). <sup>1</sup>H NMR (Fig. S6,† 400 MHz, DMSO) δ 9.14 (s, 1H), 7.80–7.37 (m, 7H), 3.75 (s, 2H), 2.42 (t, *J* = 7.3 Hz, 2H), 1.61–1.10 (m, 21H), 0.84 (t, *J* = 6.7 Hz, 3H). <sup>13</sup>C NMR (Fig. S7,† 101 MHz, DMSO) δ 166.91 (s), 156.73 (s), 142.48 (s), 138.65 (s), 136.80 (s), 131.55

(s), 130.64 (s), 129.91 (s), 129.37 (s), 124.03 (s), 116.67 (s), 35.01 (s), 34.83 (s), 31.69 (s), 31.07 (s), 29.48 (s), 29.22 (s), 29.07 (s), 29.01 (s), 28.68 (s), 22.51 (s), 14.38 (s). <sup>11</sup>B NMR (Fig. S8,† 128 MHz, DMSO) δ 0.77 (s). <sup>19</sup>F NMR (Fig. S9,† 377 MHz, DMSO) δ –133.24 (d, *J* = 26.2 Hz). HRMS (Fig. S10†), calcd for C<sub>26</sub>H<sub>36</sub>BF<sub>2</sub>NOS M<sup>–</sup>: 459.2579, found 459.2603. Elemental contents, S: 7.03% (calcd: 6.98%); B: 2.40% (calcd: 2.35%).

## 2.4. Tribological test

The antiwear capacities, last nonseizure loads (*P<sub>B</sub>* values) and welding loads (*P<sub>D</sub>* values) were evaluated on Tianji MS-10A four-ball test machine. And all steel balls are made of GCr15 material with hardness of 59–61 HRC, surface roughness of less than 0.032 μm and ball diameter of 12.7 mm. The extreme pressure properties (*P<sub>B</sub>* and *P<sub>D</sub>*) of lubricants were evaluated by the national standard method GB/T 3142-82 (similar to ASTM D2783) at 1450 rpm and room temperature for 10 seconds. The general test conditions of antiwear capacities are as follows: test temperature, 75 °C; test duration, 60 min; test rotation rate, 1200 rpm. All results were repeated at least twice. The wear degree is expressed by the mean wear scar diameter (WSD) and the mean wear volume (WV) of the three stationary balls. After tests, the WSD was obtained by measuring the wear scar diameter of three stationary balls on the microscope and measuring device of the four-ball tester. The WV was calculated by the following equation:<sup>37</sup>

$$WV = \left(\frac{\pi h}{6}\right) \left(\frac{3d^2}{4} + h^2\right)$$

where



$$h = r - \sqrt{r^2 - \frac{d^2}{4}}$$

$d$  equals the value of WSD and  $r$  (6.35 mm) is the radius of the steel ball.

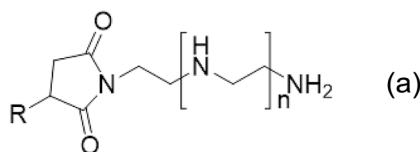
### 2.5. Antioxidation behavior analysis

Pressure differential scanning calorimetry (PDSC, NETZSCH DSC 204, Germany) can be used to determine the oxidation induction time (OIT) of lubricants to quickly evaluate their antioxidation property. The experimental process and method can be referred to our previous literatures.<sup>28,29</sup> And in this paper, PDSC tests of different lubricants were carried out in the isothermal mode at 180 °C and 500 psi oxygen pressure.

## 3. Results and discussion

### 3.1. Selection of base oil

In order to increase the solubility of additives in 150N and simulate the formulations of commercial lubricants, 150N containing 4 wt% dispersant PIBSI (PIBSI-0.04-150N) was selected as the base oil.<sup>38</sup> The main structure of dispersant PIBSI is shown in the following structure (a). And the following tests were carried out in the base oil (PIBSI-0.04-150N).



### 3.2. Antioxidation behavior

As shown in Fig. 1, the antioxidation capacity of different additives in base oil was rapidly and accurately evaluated under the isothermal mode at 180 °C and 500 psi oxygen pressure. Due to the interaction between dispersant and ZDDP in base oil,<sup>39</sup> the OIT of ZDDP in base oil (PIBSI-0.04-150N) is lower than that

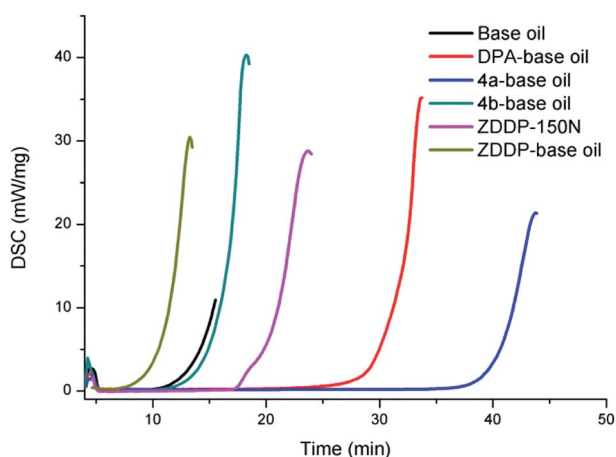


Fig. 1 Antioxidation response of different additives ( $5 \mu\text{mol g}^{-1}$ ) in base oil.

in 150N (15.6 min). Interestingly, compared with base oil and base oil containing ZDDP, the OIT of base oil containing difluoroboron derivative **4a** increased by 2.25 and 4.76 times, respectively. Compared with DPA, difluoroboron derivative **4a** exhibits superior antioxidation capacity, and its OIT increased by 32.7%. Furthermore, as expected, difluoroboron derivative **4b** almost has no effect on the antioxidation capacity of base oil. The above results of the comparisons among compounds **4a**, **4b** and DPA show that diphenylamine was the key functional group of antioxidation property. And difluoroboron derivative **4a** has better antioxidation capacity than DPA, which may be the result of the intramolecular synergism between arylamines and sulfides, which is consistent with previous research results.<sup>29,40</sup>

### 3.3. Extreme pressure performance

In order to discuss the extreme pressure properties of additive and the strength of oil film, the last nonseizure loads ( $P_B$  values) and welding loads ( $P_D$  values) were evaluated by the national standard method GB/T 3142-82 (similar to ASTM D2783), as shown in Fig. 2. The same  $P_D$  value means that additive **4a** has the same extreme pressure working ability as base oil. The  $P_B$  value of difluoroboron derivative **4a** is 804 N, which is greater than 510 N of base oil, indicating that the oil film strength of additive is higher than that of base oil. It is clearly concluded that the strength of base oil film can be significantly improved by adding difluoroboron derivative **4a**.

### 3.4. Antiwear performances

**3.4.1. Effects of additive concentration.** Initially, the antiwear performances of base oil (PIBSI-0.04-150N) with different additive concentrations were investigated by four-ball test machine under 490 N and general test conditions. The WSD changes of the novel difluoroboron derivative **4a** at different concentrations in the base oil are shown in Fig. 3. Without any additive, the WSD of base oil is as high as 0.715 mm. Adding  $2.5 \mu\text{mol g}^{-1}$  borated Schiff base **4a** to the base oil can reduce the WSD value to 0.625 mm. The maximum decrease of WSD is

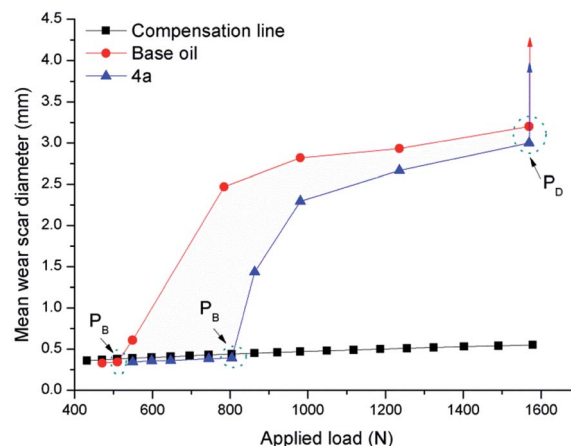


Fig. 2 The plot of  $P_B$  and  $P_D$  values for  $5 \mu\text{mol g}^{-1}$  difluoroboron derivative **4a** and base oil.





30.2% at the concentration of  $5 \mu\text{mol g}^{-1}$ , but further increase of additive concentration to 7.5 and  $10 \mu\text{mol g}^{-1}$  will increase the value of WSD, which means higher additive content would not help to improve the antiwear property. The results can be explained as follows: without additives, PIBSI is adsorbed on the steel surface to form a weak oil film. After adding the difluoroborane derivative **4a** to the base oil, the PIBSI adsorption film was replaced by additives with strong polar surface adsorption ability. With the increase of additive concentration, the PIBSI adsorptive film was gradually replaced by additives. When the additive concentration is  $5 \mu\text{mol g}^{-1}$ , the best additive adsorptive film strength and the best anti-wear effect of the lubricant formulation are obtained. However, when the concentration of additive is more than  $7.5 \mu\text{mol g}^{-1}$ , the adsorptive film of lubricant may be dominated by additives. In this case, because of the high concentration, the base oil (including PIBSI) will compete with the additives to adsorb to the metal surface, resulting in the destruction of the adsorptive film of the additives and the reduction of the wear resistance of the lubricants.<sup>41–43</sup> Considering the best wear resistance at  $5 \mu\text{mol g}^{-1}$

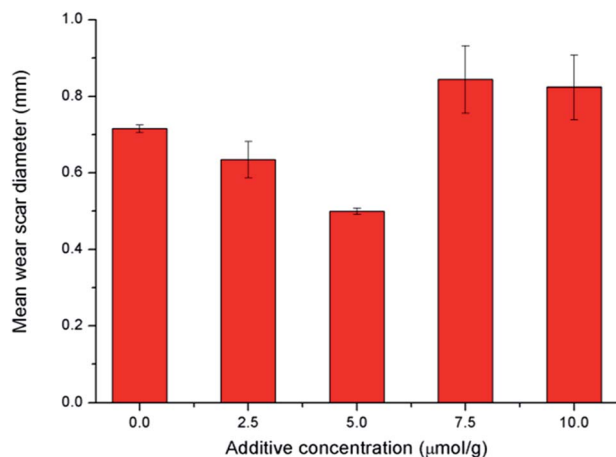


Fig. 3 Variation of the WSD for difluoroboron derivative **4a** at different concentrations in base oil.

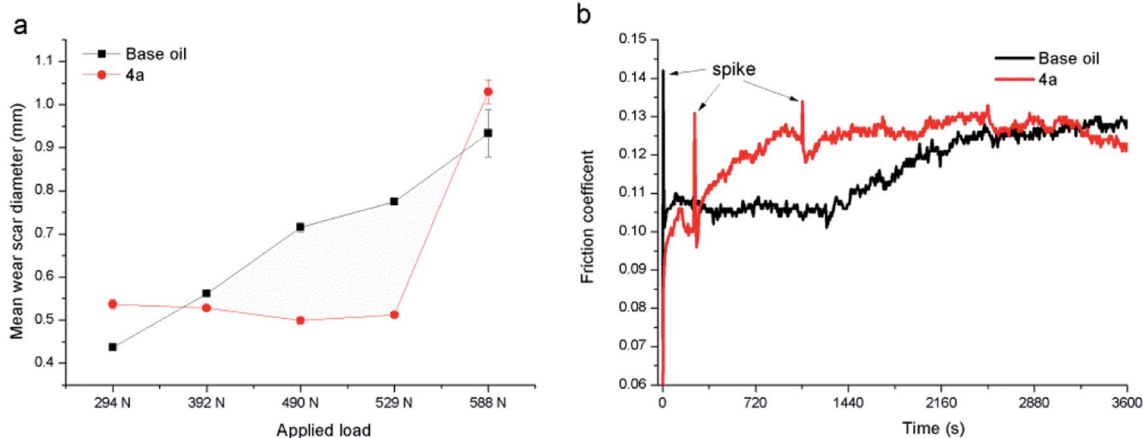


Fig. 4 (a) Variation of the WSD for difluoroboron derivative **4a** and base oil under different applied loads; and (b) friction coefficient under the load of 588 N.

concentration, all the following antiwear tests for other additives were carried out under that concentration.

**3.4.2. Effects of applied load.** As shown in Fig. 4a, the effect of applied load on antiwear performance of difluoroboron derivative **4a** was discussed. Without any additive, the WSD of the base oil increases with the increase of applied load. For the  $5 \mu\text{mol g}^{-1}$  difluoroboron derivative **4a**, the WSD remained stable under the load less than 588 N. And when the applied load is 490 N, difluoroboron derivative **4a** obtained the best antiwear performance with WSD of 0.499 mm. In order to explain the sudden increase of WSD at 588 N, the friction coefficient curve of difluoroboron derivative **4a** under 588 N is shown in Fig. 4b. The two spikes of friction coefficient curve of difluoroboron derivative **4a** indicate that the long wear under 588 N at  $75^\circ\text{C}$  destroys the additive adsorption film, which results in the abrupt increase in WSD. For base oil, the spike at the beginning of the test indicates that the adsorption film of base oil is easily destroyed under 588 N, which corresponds to the  $P_B$  results of base oil. Base on the change of antiwear performance under different applied load, 490 N is the selected applied load for the antiwear performance tests.

**3.4.3. Antiwear performance of different additives.** Fig. 5a shows the variation of the friction coefficient of steel balls, which were lubricated with the base oil (PIBSI-0.04-150N) containing different additives under 490 N and general test conditions. Due to the surface adsorption ability of the nitrogen atom in PIBSI, the friction coefficient of base oil is not less than that of  $5 \mu\text{mol g}^{-1}$  additives in base oil. The adsorption and corrosion of the fluorine make the surface of steel ball rough and increase the friction coefficients of difluoroboron derivatives **4a** and **4b**.

The antiwear performance is estimated in terms of the WSD and WV (Fig. 5b), notably, compared with the commercial ZDDP, difluoroboron derivative **4a** presents a better antiwear property with reduction of 22.8% and 64.4% on WSD and WV, respectively. And compared with base oil, the WSD (or WV) of additive **3a**, **4a**, and **4b** decreased by 12.7% (or 41.9%), 30.2% (or 76.3%) and 30.8% (or 77.1%), respectively. Moreover, compared



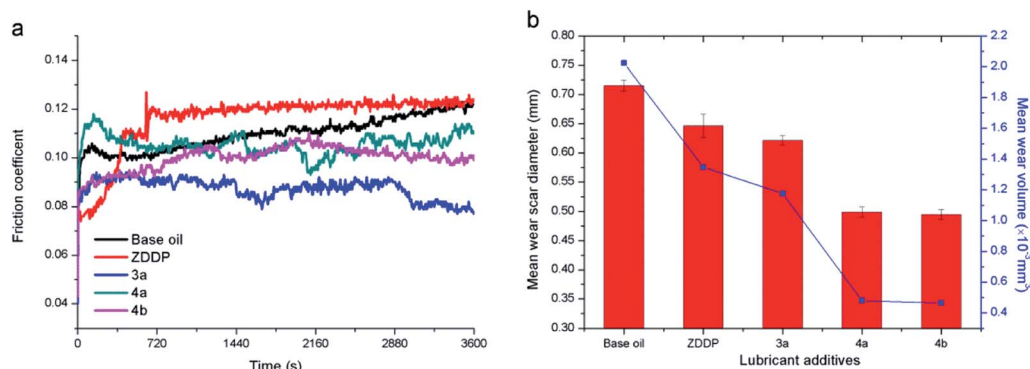


Fig. 5 Variation of the friction coefficient (a) and WSD/WV (b) for different kinds of additives in base oil, additive concentration in base oil is  $5 \mu\text{mol g}^{-1}$ .

with Schiff base **3a**, the compound **4a** exhibits excellent anti-wear property with a reduction of WSD and WV about 20.1% and 59.2%, respectively. This strong wear resistance means that the existence of boron and fluorine elements can largely improve the antiwear performance. In order to discuss the effects of diphenylamine and boron and fluorine elements functional group, comparative experiments of difluoroboron derivative **4b** were carried out. On the basis of the results, difluoroboron derivative **4a** and **4b** have good antiwear ability because of the influence of fluorine and boron, but have nothing to do with the structure of diphenylamine. The enhancement of the antiwear capability may be due to the participation of the boron and fluorine elements in tribological process and tribochemistry.<sup>14,33,44,45</sup>

### 3.5. Worn surface analysis

For better understanding the morphology and tribochemistry of worn surfaces, SEM and EDS were employed. Obviously, the metal surfaces (Fig. 6a and c) of the ball lubricated only with base oil display obvious larger wear scars and deeper furrows than those lubricated with additive **3a** (Fig. 7a and c) and

difluoroboron derivative **4a** (Fig. 8a and c). The results show that the wear and damage of the ball lubricated only with base oil are serious during the tribological process. Compared with base oil, it can be clearly seen from the elemental mapping that Schiff base **3a** is adsorbed onto the worn surface due to the surface adsorption properties of sulfur element, as shown in Fig. 7d–f. Corresponding to the better antifriction effect discussed above, Schiff base **3a** lubricating ball has smooth wear scar (Fig. 7c) because of additive's strong surface adsorption and antiwear properties. Although the difluoroborane derivative **4a** lubricating ball has grooves on the wear surface (Fig. 8c), the wear scar is smaller than that of the base oil and Schiff base **3a**, and the wear scuffing is not sharp. In addition, in Fig. 8b, the obviously detection of B (14.46 atomic%) and F (9.07 atomic%) indicates that the strong polar boron and fluorine elements of additive **4a** are transferred to the interface and formed a protective layer. Element mapping Fig. 8e and f show that B and F atoms are involved in the formation of scaly debris on wear scars, which provide intuitive evidence for the speculation of the antiwear mechanism discussed earlier. And the same wear mechanism and results are shown in the SEM images of

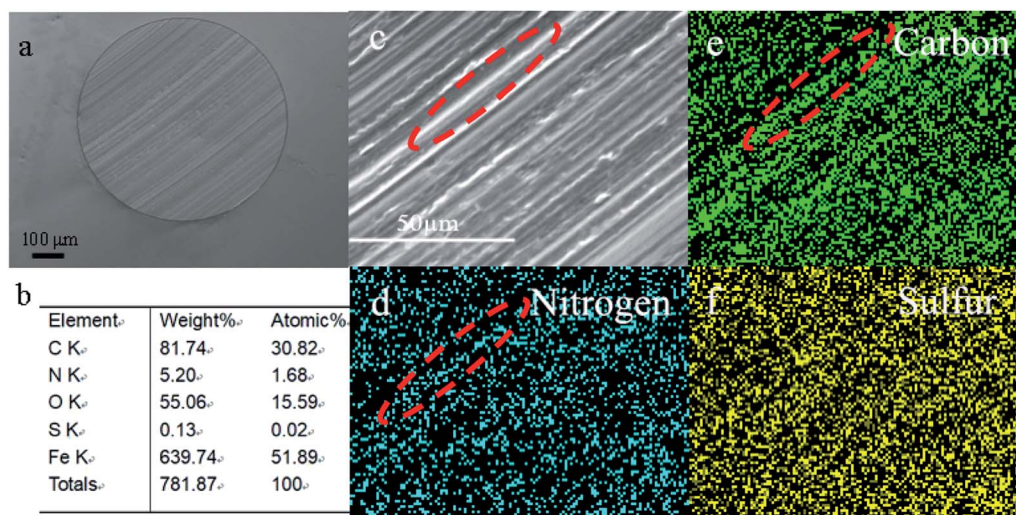


Fig. 6 SEM images (a and c), elemental content (b) and elemental mapping (d–f) of the rubbing surfaces, lubricated with base oil.





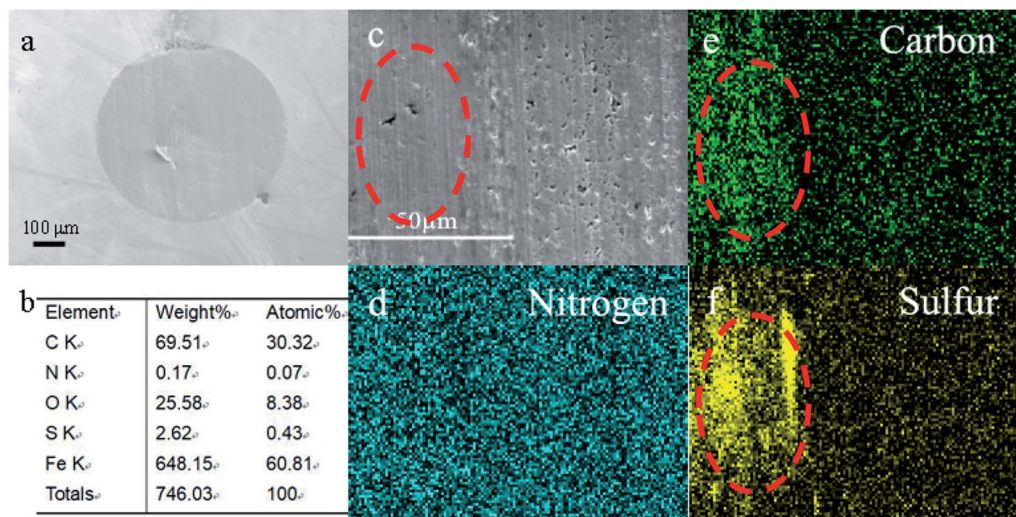


Fig. 7 SEM images (a and c), elemental content (b) and elemental mapping (d–f) of the rubbing surfaces, lubricated with Schiff base 3a.

difluoroborane derivative **4b** in Fig. S11 and S12.† It is speculated that the abrasives are formed by the exfoliation of hard compounds, which are generated by the tribochemical interaction of boron and fluorine with iron.

In order to further understand the lubrication mechanism of difluoroborane derivative **4a** in base oil, XPS was used to investigate the compositions of the worn surfaces. As shown in Fig. 9, the B 1s peak at 191.6 eV is assigned to  $B_2O_3/Fe-O-B$ , corresponding to the O 1s at 533.0 eV, which suggests that the difluoroborane derivative **4a** is degraded and reacted with oxygen during the friction process.<sup>16,41,46,47</sup> Fluorine peak at about 684.3 eV corresponds to iron fluorides. The Fe 2p<sub>3/2</sub> spectra exhibit photoelectron intensity at a binding energy consistent with  $FeF_3$  and  $Fe_2O_3$  at about 713.7 eV and 710.5 eV, respectively.<sup>33,47</sup> The peak of N 1s at 399.8 eV indicates the existence of organic nitrogen compound.<sup>16,41,48</sup> The O 1s binding energy of 529.7 eV and 531.6 eV corresponds to FeO

and C–O, respectively.<sup>42,49</sup> The composition of the boundary film, including inorganic and organic compounds, effectively improves the antiwear ability, and further confirms the participation of difluoroborane derivative **4a** in tribochemical reaction.

Based on the above results and discussions, the method of oil film formation containing difluoroborane derivative **4a** has been speculated. Without additives, PIBSI adsorbs on the steel surface to form a weak oil film. When the additive is added to the base oil at a suitable concentration ( $5 \mu\text{mol g}^{-1}$ ), the strong polar adsorption ability of additive makes the replacement of PIBSI happens and forms a tough hybrid oil film. And then, high speed (1200 rpm) and high temperature of the contact area (higher than  $150^\circ\text{C}$ ) make the additive decompose and react with iron during the antiwear process.<sup>50,51</sup> Finally, the persistent boundary film consisting of  $B_2O_3$ ,  $Fe_2O_3$ , N-containing organic compounds and iron fluoride is formed.

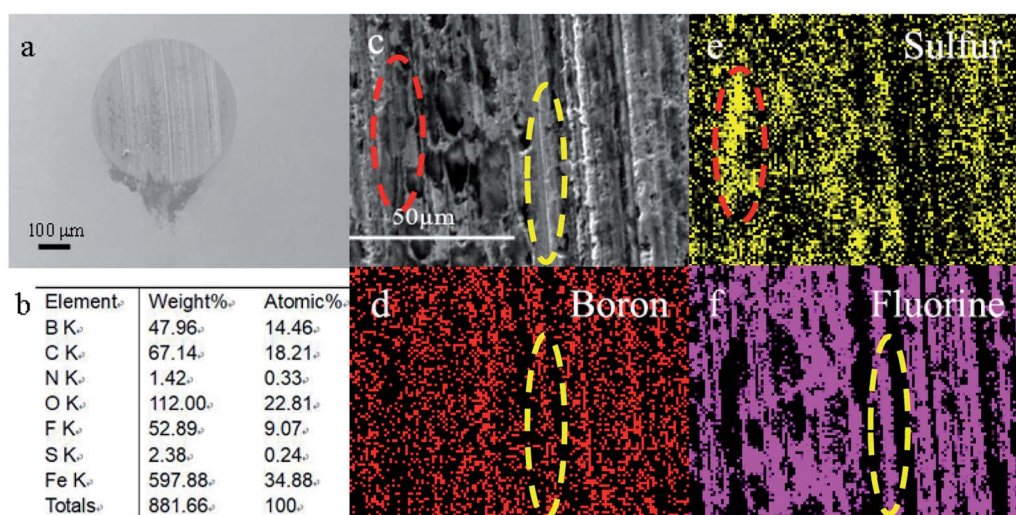


Fig. 8 SEM images (a and c), elemental content (b) and elemental mapping (d–f) of the rubbing surfaces, lubricated with difluoroborane derivative **4a**.



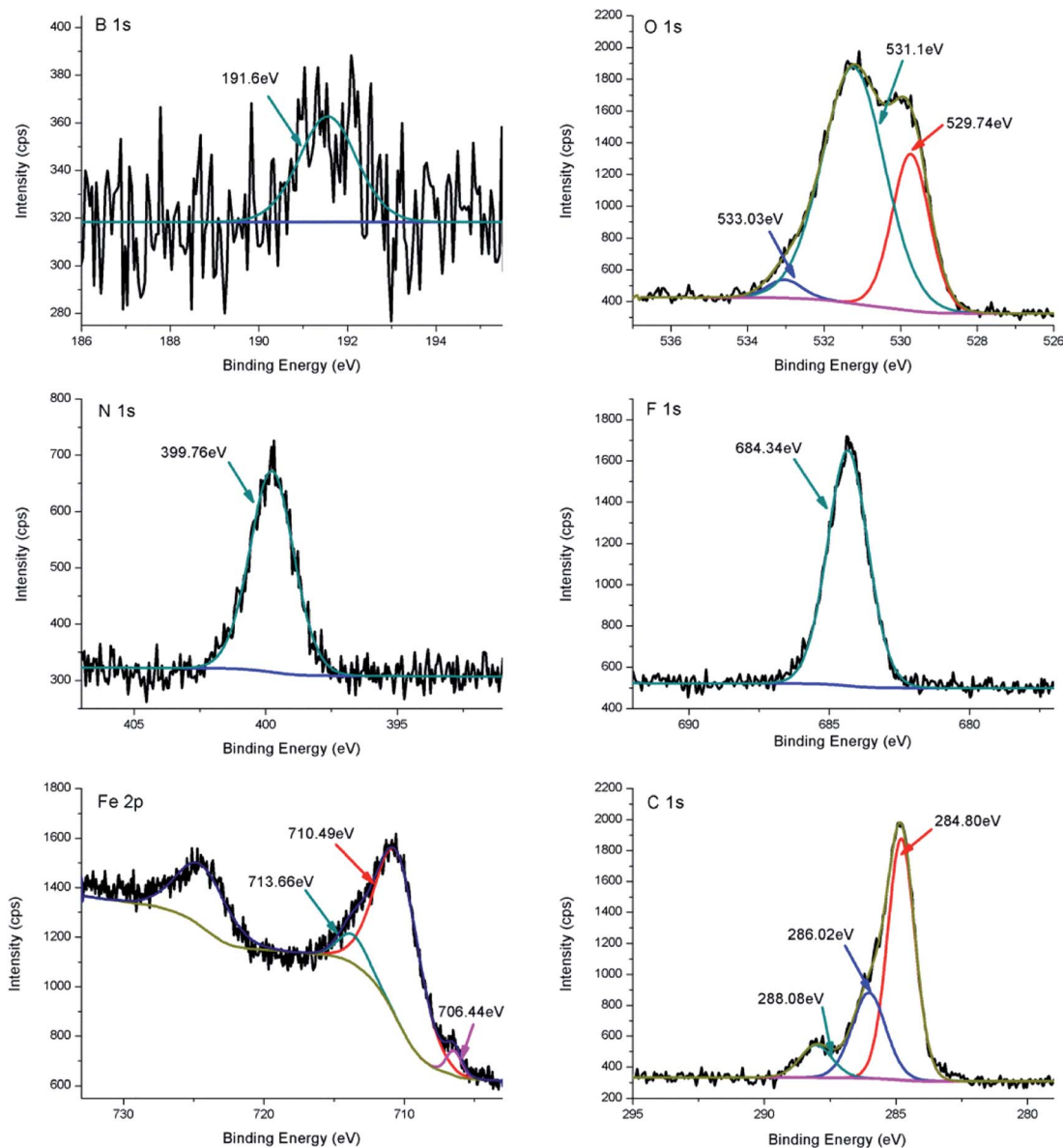


Fig. 9 XPS spectra of worn surfaces on the steel balls were lubricated by  $5 \mu\text{mol g}^{-1}$  of difluoroboron derivative **4a** in base oil.

## 4. Conclusions

Several metal-free and phosphorus-free compounds were synthesized, characterized and evaluated as lubricant additives. As a new multifunctional lubricant additive by modifying diphenylamine, the antioxidation, extreme pressure properties and antiwear properties of difluoroboron derivative **4a** were evaluated. The additive **4a** shows better antioxidation performance than base oil, traditional antioxidant DPA and **ZDDP**. And diphenylamine is the main source of antioxidation property of difluoroboron derivative **4a**. Addition of difluoroboron derivative **4a** can significantly improve the extreme pressure performance of base oil. For antiwear test, the concentration of  $5 \mu\text{mol g}^{-1}$  and 490 N was selected as additive concentration and applied load respectively. In addition, under the selected test conditions, the antiwear property of

difluoroboron derivative **4a** is better, and its mean wear volume is reduced by 76.3%, 64.4% and 59.2% compared to base oil, **ZDDP** and Schiff base **3a**, respectively. On the basis of the results, difluoroboron derivative **4a** and **4b** have good antiwear ability because of the influence of fluorine and boron, but have nothing to do with the structure of diphenylamine. The wear mechanism can be defined as abrasive wear according to the SEM and EDS results of the worn surfaces. XPS results show that the tribofilm is composed of  $\text{B}_2\text{O}_3$ ,  $\text{Fe}_2\text{O}_3$ , N-containing organic compounds and iron fluoride such as  $\text{FeF}_3$ . The composition of tribofilm reveals that difluoroboron derivative **4a** is involved in complicated tribochemical reactions and effectively improves the antiwear capacity. Therefore, as a novel metal-free and phosphorus-free multifunctional additive, the difluoroboron derivative **4a** has the potential application in lubricant.





## Conflicts of interest

There are no conflicts to declare.

## Acknowledgements

This research was supported by National Natural Science Foundation of China (Grand No. 21606247).

## References

- N. J. Mosey, M. H. Müser and T. K. Woo, *Science*, 2005, **307**, 1612–1615.
- W. Li, Y. Wu, X. Wang and W. Liu, *Lubr. Sci.*, 2011, **23**, 363–373.
- J. M. Martin, *Tribol. Lett.*, 1999, **6**, 1–8.
- H. A. Spikes, *Tribol. Lett.*, 2004, **17**, 469–489.
- H. Spikes, *Lubr. Sci.*, 2008, **20**, 103–136.
- J. L. Maurya, V. Jaiswal and R. B. Rastogi, *Proc. Inst. Mech. Eng., Part J*, 2015, **230**, 222–237.
- W. Li, C. Jiang, M. Chao and X. Wang, *ACS Sustainable Chem. Eng.*, 2014, **2**, 798–803.
- R. B. R. Kalyani and D. Kumar, *ACS Sustainable Chem. Eng.*, 2016, **4**, 3420–3428.
- R. K. Singh, A. Kukrety and A. K. Singh, *ACS Sustainable Chem. Eng.*, 2014, **2**, 1959–1967.
- M. Chao, W. Li, L. Chen and X. Wang, *Ind. Eng. Chem. Res.*, 2015, **54**, 6605–6610.
- G. Biresaw, D. Compton, K. Evans and G. B. Bantchev, *Ind. Eng. Chem. Res.*, 2016, **55**, 373–383.
- G. Biresaw, J. A. Laszlo, K. O. Evans, D. L. Compton and G. B. Bantchev, *J. Agric. Food Chem.*, 2014, **62**, 2233–2243.
- G. Yang, Z. Zhang, G. Li, J. Zhang, L. Yu and P. Zhang, *J. Tribol.*, 2011, **133**, 021801.
- R. B. Choudhary and P. P. Pande, *Lubr. Sci.*, 2010, **14**, 211–222.
- L. Wang, H. Wu, D. Zhang, G. Dong, X. Xu and Y. Xie, *Tribol. Int.*, 2018, **121**, 21–29.
- Y. Zhang, T. Cai, W. Shang, L. Sun, D. Liu, D. Tong and S. Liu, *Tribol. Int.*, 2017, **115**, 297–306.
- Y. Zhou and J. Qu, *ACS Appl. Mater. Interfaces*, 2017, **9**, 3209–3222.
- S. Shahnazar, S. Bagheri and S. B. Abd Hamid, *Int. J. Hydrogen Energy*, 2016, **41**, 3153–3170.
- M. Ye, T. Cai, W. Shang, L. Zhao, Y. Zhang, D. Liu and S. Liu, *Tribol. Int.*, 2018, **127**, 557–567.
- M. S. Charoo and M. F. Wani, *Lubr. Sci.*, 2017, **29**, 241–254.
- R. K. Singh, S. Pandey, R. C. Saxena, G. D. Thakre, N. Atray and S. S. Ray, *J. Ind. Eng. Chem.*, 2015, **26**, 149–156.
- R. K. Singh, A. Kukrety, O. P. Sharma, M. K. Poddar, N. Atray, G. D. Thakre and S. S. Ray, *Waste Biomass Valorization*, 2016, **7**, 1437–1445.
- R. K. Singh, A. Kukrety, A. K. Chatterjee, G. D. Thakre, G. M. Bahuguna, S. Saran, D. K. Adhikari and N. Atray, *Ind. Eng. Chem. Res.*, 2014, **53**, 18370–18379.
- R. K. Singh, S. Pandey, R. C. Saxena, G. D. Thakre, N. Atray and S. S. Ray, *New J. Chem.*, 2015, **39**, 5354–5359.
- Z. He, L. Xiong, F. Xie, M. Shen, S. Han, J. Hu and W. Xu, *PLoS One*, 2018, **13**, e0207267.
- M. Cai, Y. Liang, F. Zhou and W. Liu, *Wear*, 2013, **306**, 197–208.
- M. Cai, Y. Liang, M. Yao, Y. Xia, F. Zhou and W. Liu, *ACS Appl. Mater. Interfaces*, 2010, **2**, 870–876.
- S. Yu, J. Feng, T. Cai and S. Liu, *Ind. Eng. Chem. Res.*, 2017, **56**, 4196–4204.
- S. Yu and S. Liu, *Eur. J. Org. Chem.*, 2018, **2018**, 381–385.
- V. Jaiswal, K. Kalyani, R. B. Rastogi and R. Kumar, *J. Mater. Chem. A*, 2014, **2**, 10424–10434.
- K. Kalyani, V. Jaiswal, R. B. Rastogi and D. Kumar, *Proc. Inst. Mech. Eng., Part J*, 2016, **231**, 357–365.
- Z. Zheng, G. Shen, Y. Wan, L. Cao, X. Xu, Q. Yue and T. Sun, *Wear*, 1998, **222**, 135–144.
- G. Gu, Z. Wu, Z. Zhang and F. Qing, *Tribol. Int.*, 2009, **42**, 397–402.
- D. Frath, S. Azizi, G. Ulrich, P. Retailleau and R. Ziessel, *Org. Lett.*, 2011, **13**, 3414.
- J. Dobkowski, P. Wnuk, J. Buczynska, M. Pszona, G. Orzanowska, D. Frath, G. Ulrich, J. Massue, S. Mosquera-Vazquez, E. Vauthey, C. Radzewicz, R. Ziessel and J. Waluk, *Chemistry*, 2015, **21**, 1312–1327.
- C. Huang and J. T. Loper, *US Pat.*, US2008188385-A1, 2008.
- D. Berman, A. Erdemir and A. V. Sumant, *Carbon*, 2013, **59**, 167–175.
- Y. Zhang, X. Zeng, H. Wu, Z. Li, T. Ren and Y. Zhao, *Tribol. Lett.*, 2014, **53**, 533–542.
- M. Shiomi, M. Tokashiki, H. Tomizawa and T. Kuribayashi, *Lubr. Sci.*, 2010, **1**, 131–147.
- J. B. He, H. Shi, Y. Wang and X. L. Gao, *Molecules*, 2018, **23**, 1–8.
- F. Jin, G. Yang, Y. Peng, S. Zhang, L. Yu and P. Zhang, *Lubr. Sci.*, 2016, **28**, 505–519.
- V. Jaiswal, S. R. Gupta, R. B. Rastogi, R. Kumar and V. P. Singh, *J. Mater. Chem. A*, 2015, **3**, 5092–5109.
- A. Sammaiah, K. V. Padmaja, S. S. Kaki and R. B. N. Prasad, *RSC Adv.*, 2015, **5**, 77538–77544.
- Y. Shi and J. Dong, *Lubr. Sci.*, 2000, **12**, 357–361.
- R. B. Rastogi, J. L. Maurya and V. Jaiswal, *Tribol. Trans.*, 2013, **56**, 592–606.
- H. Zhongyi, X. Liping, Q. Liang, H. Sheng, C. Aixi, Q. Jianwei and F. Xisheng, *Lubr. Sci.*, 2014, **26**, 81–94.
- D. D. Hawn and B. M. Dekoven, *Surf. Interface Anal.*, 1987, **10**, 63–74.
- G. Yang, J. Zhao, L. Cui, S. Song, S. Zhang, L. Yu and P. Zhang, *RSC Adv.*, 2017, **7**, 7944–7953.
- Y. Liu, P. Liu, L. Che, C. Shu and X. Lu, *Chin. Sci. Bull.*, 2012, **57**, 4641–4645.
- F. Spadaro, A. Rossi, E. Lainé, P. Woodward and N. D. Spencer, *Tribol. Lett.*, 2016, **65**, 11.
- S. Q. A. Rizvi, *A comprehensive review of lubricant chemistry, technology, selection, and design*, Library of Congress Cataloging-in-Publication Data, ASTM International, Baltimore, 2009.

